Inorg. Chem. **2008**, *47*, 10554−10564

Strong Intramolecular Si−N Interactions in the Chlorosilanes $Cl_{3-n}H_nSiOCH_2CH_2NMe_2$ ($n = 1-3$)

Michael Hagemann,[‡,§] Andreas Mix,[‡] Raphael J. F. Berger,[‡] Tania Pape,[†] and Norbert W. Mitzel*[,‡,§]

Institut für Anorganische and Analytische Chemie, Westfälische Wilhelms−Universität Münster, Corrensstrasse 30/36, 48149 Münster, Germany, Fakultät für Chemie, Universität Bielefeld, Universitätsstrasse 25, D-33615 Bielefeld, Germany, and International Graduate School of Chemistry, Münster, Corrensstrasse 30, D-48149 Münster, Germany

Received June 30, 2008

The compounds $Cl_3SiOCH_2CH_2NMe_2$ (**1**) and $Cl_2HSiOCH_2CH_2NMe_2$ (**2**) were prepared by reactions of lithium 2-(dimethylamino)ethanolate with $SiCl_4$ and $HSiCl_3$. The analogous reaction with H_2SiCl_2 gave $ClH_2SiOCH_2CH_2NMe_2$ (**3**), but only in a mixture with $Cl_2HSiOCH_2CH_2NMe_2$ (**2**), from which it could not be separated. All compounds were characterized by IR and NMR (^1H, ^{13}C, ^{29}Si) spectroscopy, **1** and **2** by elemental analyses and by determination of their crystal structures. $Cl_3SiOCH_2CH_2NMe_2$ (**1**) and $Cl_2HSiOCH_2CH_2NMe_2$ (**2**) crystallize as monomeric ring compounds with pentacoordinate silicon atoms participating in intramolecular Si−N bonds [2.060(2) Å (**1**), 2.037(2) Å (**2**)]. The dative bonds in **1** and **2** between the silicon and nitrogen atoms could also be proven to exist at low temperatures in solution in ^1H,^{29}Si-HMBC-NMR experiments by detection of the scalar coupling between the ^{29}Si and the protons of the NCH_2 and NCH_3 groups. A function describing the chemical shift $\delta_{exp}{}^{29}Si$ dependent on the chemical shifts of the individual equilibrium components, the temperature, and the free enthalpy of reaction was worked out and fitted to the experimental VT-NMR data of **1** and **2**. This provided values of the free reaction enthalpies of $\Delta G = -28.8 \pm 3.9$ kJ·mol^{-1} for **1** and $\Delta G = -22.3 \pm 0.4$ kJ·mol^{-1} for **2** and estimates for the chemical shifts of open-chain (index o) and ring conformers (index r) for **1** of $\delta_r = -94 \pm 2$ ppm and $\delta_o = -36 \pm 5$ ppm and for **2** of $\delta_r = -82 \pm 1$ ppm and $\delta_o = -33 \pm 4$ ppm. The value of δ_r for **1** is very close to that obtained from a solid-state ^{29}Si MAS NMR spectrum. Quantumchemical calculations (up to MP2/TZVPP) gave largely differing geometries for **1** (with a Si···N distance of 3.072 Å), but well reproduced the geometry of **2**. These differences are due to Cl···H and Cl···C repulsions and solid state effects, which can be modeled by conductor-like screening model calculations and also rationalized in terms of the topology of the electron density, which was analyzed in terms of the quantum theory of atoms in molecules.

Introduction

There is a large body of knowledge about hypercoordinate silicon compounds.[1,2] To a large fraction, this comprises compounds with intramolecular dative Si−N bonds. In this context, different ring sizes have been investigated, and the smallest, three-membered rings are of particular importance, as they are quoted as the basis for the explanation of the so-called α effect.[3] In this context, the picture of a three-membered ring with a dative Si···X interaction (X = donor atom) is used to explain the high hydrolysis rates of the Si−O functions in compounds of the type $(RO)_3SiCH_2X$. However, in a series of recent studies, such a structural feature of a three-membered ring for SiCN units could not be found[4,5] even though highly electronegative substituents were bonded to the silicon atom. Even for $F_3SiCH_2NMe_2$[5] there is no evidence of a significant attractive Si···N interaction in the monomers in the gas phase [$\angle$(SiCN) = 110.3(7)°, d(Si···N) = 2.723 Å], while the compound dimerizes in the solid state

* Author to whom correspondence should be addressed. E-mail: mitzel@uni-bielefeld.de.
† Westfälische Wilhelms−Universität Münster.
‡ Universität Bielefeld.
§ International Graduate School of Chemistry.

(1) (a) Chuit, C.; Corriu, R. J. P.; Reye, C.; Young, J. C. *Chem. Rev.* **1993**, *93*, 1371. (b) Kost, D.; Kalikman, I.; Rappoport, Z.; Apeloig, Y. *The Chemistry of Organosilicon Compounds*; Wiley: New York, 1998; Vol. 2, pp 1339−1445. (c) Corriu, R. J. P.; Young, J. C.; Patai, S.; Rappoport, Z.; Apeloig, Y. *The Chemistry of Organic Silicon Compounds*; Wiley: New York, 1989; pp. 1241−1288. (d) Schoeller, W.; Rozhenko, A. *Eur. J. Inorg. Chem.* **2000**, 375.

10.1021/ic801205q CCC: $40.75
Published on Web 10/11/2008

by two Si···N interactions to give a six-membered ring. Exchange of the bridging CH_2 unit between Si and N atoms by an isoelectronic O atom leads to dramatically changed properties in such compounds. The bending potential of the Si−O−N angle is much flatter than that of a corresponding Si−C−N angle. As a result, very acute Si−O−N angles and short Si−N distances are found in these hydroxylaminosilanes. The most extreme cases were observed in the solid state for $H_2Si(ONMe_2)_2$,[6] $ClH_2SiONMe_2$,[7] $F_3SiONMe_2$,[8] and $(F_3C)F_2SiONMe_2$.[9] In the latter, the Si−O−N angle adopts a value of 74.1(1)°, and a Si−N distance of only 1.904(2) Å is found, which is less than the Si−C bond length at 1.912(1) Å.

Examples for longer chains between silicon and donor atoms are numerous,[1,2,10] but simple examples with fully flexible linking units (not involved in benzene rings etc.) are still not well investigated. Again, such compounds, in particular such with a donor function in the δ position relative to the silicon atom, are of significant industrial importance (surface mediators, adhesive agents, cross-linkers, etc.).[11,3d] The bridging unit generally comprises a propylene unit ($-CH_2-CH_2-CH_2-$), which on one hand is responsible for the high flexibility of the molecular backbone and on the other enables the formation of Si···N contacts, leading to ring closure and penta-coordination of the silicon atom, which is seen as the reactive center in the hydrolysis reactions of $(RO)_3Si(CH_2)_3X$ compounds.[12]

In order to compare the simplest systems with one another and to rule out complicated substituent effects, we recently investigated $H_3SiCH_2CH_2CH_2NMe_2$, which is a five-membered ring in the solid state but a complicated mixture of different conformers in the gas phase, with a ring conformer contribution being only 24% at ambient temperature. This example shows that even in molecules without strongly electronegative substituents at the silicon atom a direct interaction between silicon and the nitrogen atoms exists and can dominate the structures and properties of these compounds.[13]

In this contribution, we report on compounds with $SiOCH_2CH_2N$ backbones, for which to the best of our knowledge no structural data on simple examples exist, that is, with silicon atoms substituted only by small functional groups such as F, Cl, or H atoms or methyl groups. $F_3SiOCH_2CH_2NMe_2$ was earlier synthesized by two different routes: by Schmutzler et al., who reacted $Me_3SiOCH_2CH_2NMe_2$ with SiF_4 under the liberation of Me_3SiF,[14] and by Voronkov et al., who reacted $C_6H_5SiF_3$ with $HOCH_2CH_2NMe_2$ under the formation of $F_3SiOCH_2CH_2NMe_2$ and benzene.[15] Here, we present results on silanes of the formula $Cl_{3-x}H_xSiOCH_2CH_2NMe_2$, in particular with respect to the molecular and electronic structure and the equilibria between open-chain and ring conformers.

Experimental Section

All operations were carried out under a dry and oxygen-free nitrogen atmosphere using standard Schlenk and glovebox techniques. All solvents were dried and saturated with nitrogen by standard methods and freshly distilled prior to use. $SiCl_4$, $HSiCl_3$, Me_3SiCl Me_2SiCl_2, and 2-(dimethylamino)ethanol were purchased from a commercial source and used after distillation.

NMR spectra were recorded on Bruker AC 200, Bruker AV 400 NMR, and Bruker Avance 600 spectrometers. Chemical shifts are reported in parts per million with reference to the residual solvent signals for ^1H and ^{13}C NMR spectroscopy and to external $SiMe_4$ for ^{29}Si NMR spectroscopy. Abbreviations for NMR data: s = singlet, d = doublet, t = triplet, q = quartet, and m = multiplet. Elemental analyses were carried out on a VARIO El III CHNS instrument. IR spectra were recorded on a Midac Prospect IR spectrometer. Abbreviations for IR data: vs = very strong, s = strong, m = medium, and w = weak. Solid compounds were measured as a Nujol mull; volatile compounds were analyzed in the gas phase. Mass spectra were recorded on a Varian MAT 212 instrument.

$LiOCH_2CH_2NMe_2$. 2-(Dimethylamino)ethanol (11.5 g, 129 mmol) was dissolved in diethyl ether (60 mL) and cooled to −78 °C. At this temperature, *n*-butyl lithium (81 mL, 130 mmol, 1.6 M in hexane) was slowly added. Within 14 h, the reaction mixture was allowed to warm to ambient temperature. The solvent was removed under reduced pressure; the reaction product was dried in a vacuum and stored in a refrigerator within a glovebox at −25 °C.

$Cl_3SiOCH_2CH_2NMe_2$ (1). Tetrachlorosilane (49.7 g, 292 mmol) was dissolved in hexane (80 mL) and cooled to −40 °C. $LiOCH_2CH_2NMe_2$ (25.5 g, 265 mmol) was suspended in diethyl ether and dropped slowly into the cooled tetrachlorosilane solution. Within 14 h, the reaction mixture was allowed to warm to room temperature (RT). The solid byproduct was filtered off and washed with hexane. The combined solutions were concentrated in a vacuum, leading to precipitation of the product. Recrystallization from THF afforded a pure product as a colorless solid (7.02 g, 32 mmol, 12%). Single crystals for X-ray diffraction experiments were

(2) Brook, M. A.; *Silicon in Organic, Organometallic and Polymer Chemistry*, 1st ed.; Wiley VCH: New York, 2000.
(3) Bauer, A.; Kammel, T.; Pachaly, B.; Schäfer, O.; Schindler, W.; Stanjek, V.; Weis, J. In *Organosilicon chemistry V*; Auner, N., Weis, J. Eds.; Wiley-VCH: Weinheim, Germany, 2003; p 527. (b) Kostyanovskii, R. G.; Prokof'ev, A. K. *Dokl. Akad. Nauk SSSR* **1965**, *164*, 1054. (c) One Step Ahead - Organofunctional Silanes from Wacker:http://www.wacker.com/internet/webcache/de_DE/_Downloads/GENIOSIL_Brosch_en.pdf (accessed Sep 2008). (d) Giessler, S.; Standke, B. *Farbe und Lack* **2005**, *4*, 134. (e) *A Guide to Silane Solutions from Dow Corning*. http://www.dowcorning.com/content/publishedlit/SILANE-GUIDE.pdf (accessed Sep 2008).
(4) Mitzel, N. W.; Kiener, C.; Rankin, D. W. H. *Organometallics* **1999**, *18*, 3437.
(5) Mitzel, N. W.; Vojinović, K.; Foerster, T.; Robertson, H. E.; Borisenko, K. B.; Rankin, D. W. H. *Chem.—Eur. J.* **2005**, *11*, 5114.
(6) (a) Mitzel, N. W.; Losehand, U. *Angew. Chem.* **1997**, *109*, 2897. (b) Mitzel, N. W.; Losehand, U. *Angew. Chem., Int. Ed. Engl.* **1997**, *36*, 2807. (c) Losehand, U.; Mitzel, N. W. *Inorg. Chem.* **1998**, *37*, 3175.
(7) Mitzel, N. W.; Losehand, U. *J. Am. Chem. Soc.* **1998**, *120*, 732.
(8) Mitzel, N. W.; Losehand, U.; Wu, A.; Cremer, D.; Rankin, D. W. H. *J. Am. Chem. Soc.* **2000**, *122*, 447.
(9) Mitzel, N. W.; Vojinović, K.; Fröhlich, R.; Foerster, T.; Robertson, H. E.; Borisenko, K. B.; Rankin, D. W. H. *J. Am. Chem. Soc.* **2005**, *127*, 13705.
(10) Akiba, K.-Y. *Chemistry of Hypervalent Compounds*; Wiley-VCH, Inc.: New York, 1999.
(11) Deschler, U. *Angew. Chem., Int. Ed. Engl.* **1986**, *25*, 236.
(12) Deiters, J. A.; Holmes, R. R. *J. Am. Chem. Soc.* **1990**, *112*, 7197.
(13) Hagemann, M.; Berger, R. J. F.; Hayes, S. A.; Stammler H.-G.; Mitzel, N. W. *Chem.—Eur. J.* **2008**, In press.
(14) Krebs, R.; Schomburg, D.; Schmutzler, R. *Z. Naturforsch.* **1985**, *40b*, 282.
(15) Voronkov, M. G.; Grebneva, E. A.; Trofimova, O. M.; Chernov, N. F.; Albanov, A. I.; Chipanina, N. N. *Dokl. Chem.* **2006**, *409*, 139.

grown by slowly cooling a saturated THF solution of **1** to −78 °C. Anal. calcd for $C_4H_{10}Cl_3NOSi$ (222.6 g·mol^{-1}): C, 21.50; N, 6.29; H, 4.53%. Found: C, 21.31; N, 6.30; H, 4.64%. FT-IR (Nujol mull) ν [cm^{-1}]: 2972 (s, ν(CH)), 2850 (s, ν(CH)), 1462 (vs), 1377 (m), 1367 (m), 1231 (w), 1109 (m), 1072 (m), 1001 (w), 947 (w), 722 (w), 596 (w). ^{1}H NMR (400 MHz, C_6D_6, 25 °C): δ 1.90 (s, 6H, $^1J_{CH}$ = 134 Hz, N(CH_3)$_2$), 2.12 (t, 2H, $^3J_{HH}$ = 6.0 Hz, NCH_2), 3.50 (t, 2H, $^3J_{HH}$ = 6.0 Hz, CH_2O). ^{13}C NMR (100 MHz, C_6D_6, 25 °C): δ 45.4 (q, $^1J_{CH}$ = 137 Hz, $^3J_{CH}$ = 4.5 Hz, N(CH_3)$_2$), 57.2 (t, $^1J_{CH}$ = 139 Hz, $^3J_{CH}$ = 6.0 Hz, NCH_2), 61.2 (t, $^1J_{CH}$ = 149 Hz, $^3J_{CH}$ = 6.0 Hz, OCH_2). ^{29}Si DEPT-19.5 NMR (79.5 MHz, C_6D_6): δ −72. ^{29}Si MAS NMR (59.6 MHz, 4 kHz): δ −95.3. MS (EI; *m*/*z*): 221 (M^+, 7%), 186 (M^+ − Cl, 4%), 170 (M^+ − Cl − CH_3, 100%), 133 ($SiCl_3^+$, 84%), 58 ($(CH_3)_2NCH_2^+$, 87%)

$Cl_2HSiOCH_2CH_2NMe_2$ (2). A solution of trichlorosilane (10.7 g, 80 mmol) in pentane (40 mL) was cooled to −25 °C. $LiOCH_2CH_2NMe_2$ (5.7 g, 60 mmol) was suspended in pentane and dropped slowly into the trichlorosilane solution. Within 14 h, the reaction mixture was allowed to warm to room temperature. The solid byproduct was filtered off and washed with diethyl ether. The solvent of the combined solutions was removed under reduced pressure. Recrystallization from THF afforded a pure product as a colorless solid (3.01 g, 16 mmol, 20%). Single crystals for X-ray diffraction experiments were grown by slowly cooling a saturated solution in THF of **2** to −78 °C. Anal. calcd for $C_4H_{11}Cl_2NOSi$ (188.1 g·mol^{-1}): C, 25.54; N, 7.45; H, 5.89%. Found: C, 26.08; N, 7.07; H, 6.22%. ^{1}H NMR (400 MHz, C_6D_6, 25 °C): δ 1.66 (s, 6H, $^1J_{CH}$ = 138 Hz, N(CH_3)$_2$), 1.98 (t, 2H, $^3J_{HH}$ = 6.1 Hz, NCH_2), 3.41 (t, 2H, $^1J_{CH}$ = 148 Hz, $^3J_{HH}$ = 6.1 Hz, CH_2O), 5.65 (s, 1H, $SiCl_2H$). ^{13}C NMR (100 MHz, C_6D_6, 25 °C): δ 43.6 (q, $^1J_{CH}$ = 138 Hz, $^3J_{CH}$ = 4.3 Hz, N(CH_3)$_2$), 55.5 (t, $^1J_{CH}$ = 136 Hz, $^3J_{CH}$ = 4.2 Hz, NCH_2), 59.5 (t, $^1J_{CH}$ = 149 Hz, OCH_2). ^{29}Si DEPT-19.5-NMR (79.5 MHz, C_6D_6): δ −75 ($^1J_{SiH}$ = 376 Hz, O*Si*Cl_2H).

$ClH_2SiOCH_2CH_2NMe_2$ (3). Dichlorosilane (6 mL, approximately 60 mmol) was condensed into a vessel held at −78 °C, which was connected to a dropping funnel containing a suspension of $LiOCH_2CH_2NMe_2$ (4.75 g, 50 mmol) in diethyl ether (60 mL). The suspension was slowly added to the silane at −78 °C. Within 14 h, the reaction mixture was allowed to warm to room temperature. The excess of silane was evaporated through a bubbler by gentle expulsion with nitrogen. The solid byproduct was filtered off and washed with diethyl ether. The solvent of the combined solutions was removed under reduced pressure. NMR analyses showed the formation of the desired product and of $Cl_2HSiOCH_2CH_2NMe_2$. Both products crystallize readily, so that we were not able to separate $ClH_2SiOCH_2CH_2NMe_2$ and $Cl_2HSiOCH_2CH_2NMe_2$, even after repeated attempts of fractional crystallization (five times). The following data refer to the signals of **3** detected besides those of **2**. ^{1}H NMR (400 MHz, C_6D_6, 25 °C): δ 1.46 (s, 6H, $^1J_{CH}$ = 137 Hz, NCH_3), 1.74 (t, 2H, $^3J_{HH}$ = 5.9 Hz, NCH_2), 3.34 (t, 2H, $^3J_{HH}$ = 5.9 Hz, OCH_2), 5.15 (s, 2H, $^1J_{SiH}$ = 292 Hz, SiH_2). ^{13}C NMR (100 MHz, C_6D_6, 25 °C): δ 43.0 (NCH_3), 57.1 (NCH_2), 59.3 (OCH_2). ^{29}Si DEPT-19.5-NMR (79.5 MHz, C_6D_6) δ −71 ($^1J_{SiH}$ = 293 Hz, O*Si*H_2Cl).

$Cl_2HSiOCH_2CH_3$. *n*-Butyl lithium (74 mL, 1.6 molar solution in hexane, 118 mmol) was slowly added to a solution of dry ethanol (5.44 g, 118 mmol) in pentane (50 mL) cooled to 0 °C. At this temperature, a colorless solid formed. The solvent was removed under reduced pressure to yield the colorless solid ($LiOCH_2CH_3$). Trichlorosilane (16.0 g, 118 mmol) was dissolved in THF (100 mL) and cooled to −78 °C. In a dropping funnel with a stirrer, $LiOCH_2CH_3$ was suspended in THF (40 mL) and slowly added to the cooled solution (−78 °C). The reaction solution was stirred for 14 h. After that, the product was isolated by fractional distillation at 90 °C and 50 mbar. $C_2H_6Cl_2OSi$ (145.6 g·mol^{-1}). ^{1}H NMR (400 MHz, C_6D_6, 25 °C): δ 1.04 (t, 3H, $^3J_{HH}$ = 7.02 Hz, CH_3), 3.69 (q, 2H, $^3J_{HH}$ = 7.02 Hz, CH_2), 5.01 (s, $^1J_{SiH}$ = 325 Hz, Si*H*). ^{13}C NMR (100 MHz, C_6D_6, 25 °C): δ 17.9 (CH_3), 59.6 (CH_2). ^{29}Si DEPT-30-NMR (79.5 MHz, C_6D_6): δ −48 ($^1J_{SiH}$ = 325.6 Hz). FT-IR (gas) ν [cm^{-1}]: 519 (m), 829 (s), 866 (s), 974 (m), 1170 (s), 1394 (m), 2232 (s, υ(Si−H)), 2849 (m).

Table 1. Crystal Data and Structure Refinement Parameters for $Cl_3SiOCH_2CH_2NMe_2$ (**1**) and $Cl_2HSiOCH_2CH_2NMe_2$ (**2**)

	$Cl_3SiOCH_2CH_2NMe_2$ (**1**)	$Cl_2HSiOCH_2CH_2NMe_2$ (**2**)
chemical formula	$C_4H_{10}Cl_3NOSi$	$C_4H_{11}Cl_2NOSi$
fw	222.57	188.13
cryst syst/space group	monoclinic/*Cc*	orthorhombic/*Pbca*
a (Å)	6.3951(9)	12.255(3)
b (Å)	13.1988(13)	10.586(2)
c (Å)	10.6253(15)	13.043(3)
β (deg)	92.521(3)	90
V (Å^{-3})	896.0(2)	1692.2(6)
Z	4	8
T (K)	153(2)	163(2)
ρ_{calcd} (g cm^{-3})	1.650	1.477
λ (Å)/μ (mm^{-1})	0.71073/1.093	0.71073/0.837
Θ range for data collection	3.1−30.0°	4.5−27.1°
reflns collected/independent	5021/2496	24757/1821
completeness to Θ	99.5%	98.0%
obsd reflns	2438	1466
data/restraints/params	2496/2/93	1821/0/2
GOF on F^2	1.945	1.114
R1, wR2 [$I < 2\sigma(I)$]	0.0233/0.0554	0.0295/0.0664
R1, wR2 (all data)	0.0241/0.0558	0.0433/0.0715
largest diff peak/hole (*e* Å^{-3})	0.269/−0.201	0.368/−0.332

Crystal Structures. Single crystals suitable for X-ray diffraction were coated with oil and mounted on top of a glass fiber. Diffraction data for **1** were collected with a Bruker AXS APEX CCD diffractometer equipped with a rotating anode at 153(2) K using graphite monochromatic Mo Kα radiation (λ = 0.71073 Å). They were collected over the full sphere and were corrected for absorption. Diffraction data for **2** were collected with a STOE IPDS 1 equipped with an image plate system at 163(2) K using graphite monochromatic Mo Kα radiation.

The structures were solved by direct methods and were refined by full-matrix least-squares techniques against F_o^2 with SHELXTL 5.01.[16] All non-hydrogen atoms were refined anisotropically. The hydrogen atom of the Si−H function in **2** was not included in the refinements, and all other hydrogen atoms were included in calculated positions and refined in a riding model. Details of the crystal structure analyses are listed in Table 1.

Crystallographic data (excluding structure factors) for the structures reported in this paper have been deposited with the Cambridge Crystallographic Data Centre as supplementary publications CCDC-693201 (**1**) and CCDC-693202 (**2**). Copies of the data can be obtained from CCDC, 12 Union Road, Cambridge CB2 1EZ, U.K. (fax: (+44)1223−336−033; e-mail: deposit@ccdc.cam.ac.uk).

Results and Discussion

Synthesis and Characterization. The compounds $Cl_3SiOCH_2CH_2NMe_2$ (**1**), $Cl_2HSiOCH_2CH_2NMe_2$ (**2**), and $ClH_2SiOCH_2CH_2NMe_2$ (**3**) were prepared by the reactions of suspensions of $LiOCH_2CH_2NMe_2$ with the corresponding chlorosilanes (Scheme 1). $LiOCH_2CH_2NMe_2$ was generated

(16) (a) *SHELXTL-PC 5.1*; Siemens Analytical X-Ray Instruments Inc.: Madison, WI, 1990. (b) Sheldrick, G. M. *SHELXL-97*; Universität Göttingen: Göttingen, Germany, 1997.

Scheme 1

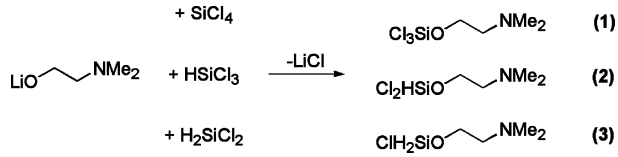

by the reaction of the *N*,*N*-dimethylaminoethanol $HOCH_2CH_2NMe_2$ with *n*-butyl lithium.

The resulting 2-(dimethylamino)ethoxy-substituted silanes are soluble in ethereal solvents but only sparingly soluble in alkanes. Compounds **1** and **2** are solids at room temperature, with melting points of 90 and 65 °C, respectively. They have been identified by IR and NMR spectroscopy (see below), by mass spectrometry, and by elemental analysis and determination of their solid-state structures accomplished by X-ray diffraction. For this purpose, single crystals of **1** and **2** were grown by cooling saturated solutions in THF slowly to −78 °C.

The synthesis of **3** also yielded **2** as a byproduct. Since the properties of both compounds are similar, **3** could not be isolated from these mixtures. Repeated fractional crystallization (five times) always yielded single crystals of **2**. However, the existence of **3** could without a doubt be confirmed by multinuclear NMR spectroscopy.

Crystal Structures. Compounds **1** and **2** can easily be obtained as single crystalline material from ethers and alkanes by cooling their saturated solutions. Compound **2** crystallized even at the wall of a frit during workup of the reaction mixture. Figures 1 and 2 depict the molecular structures of **1** and **2** in the crystals, and Table 2 contains a list of selected structural parameters for comparison together with the results of quantumchemical calculations discussed below.

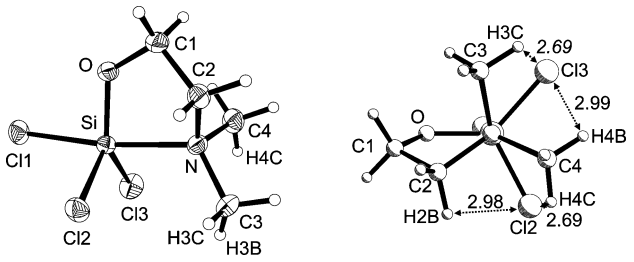

Figure 1. Molecular structure of compound $Cl_3SiOCH_2CH_2NMe_2$ (**1**). The probability of the depicted ellipsoids is 50% (left plot). The right plot shows a view along the N−Si vector and gives the lengths of short Cl···H contacts in angstroms.

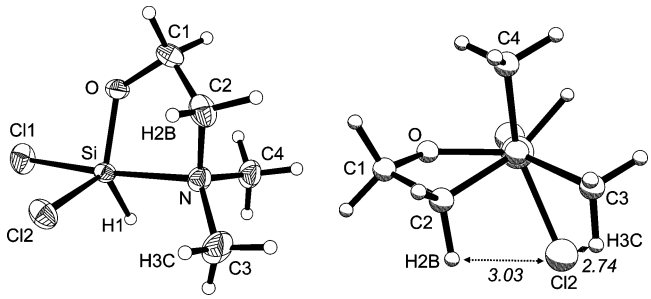

Figure 2. Molecular structure of compound $Cl_2HSiOCH_2CH_2NMe_2$ (**2**). The probability of the depicted ellipsoids is 50% (left plot). The right plot shows a view along the N−Si-vector and gives the lengths of short Cl···H contacts in angstroms.

Table 2. Selected Bond Lengths [Å] and Angles [deg] for $Cl_3SiOCH_2CH_2NMe_2$ (**1**) and $Cl_2HSiOCH_2CH_2NMe_2$ (**2**) As Determined by Low-Temperature X-Ray Crystallography (XRD) and by Quantum Chemical Methods at the (RI)MP2/TZVPP (MP2) Level of Theory and Using the Conductor-Like Screening Model (COSMO) at This Theory Level (Cosmo)

	1			**2**	
	XRD	MP2	Cosmo	XRD	MP2
Si−N	2.060(1)	3.072	2.032	2.037(2)	2.235
Si−Cl1	2.157(1)	2.042	2.163	2.180(1)	2.102
Si−Cl2	2.072(1)	2.038	2.083	2.073(1)	2.082
Si−Cl3/H1	2.073(1)	2.041	2.092	1.39(2)	1.472
Si−O	1.637(1)	1.624	1.660	1.647(2)	1.663
C1−O	1.426(2)	1.424	1.428	1.435(2)	1.413
C1−C2	1.519(2)	1.512	1.514	1.510(3)	1.523
C2−N	1.489(2)	1.453	1.478	1.484(3)	1.462
C3−N	1.489(2)	1.454	1.477	1.486(2)	1.465
C4−N	1.498(2)	1.455	1.488	1.489(2)	1.469
N−Si−Cl1	172.0(1)	172.5	172.1	170.8(1)	171.8
N−Si−Cl2	92.3(1)	76.5	92.0	93.5(1)	88.2
N−Si−Cl3/H1	89.0(1)	78.5	88.5	86.7(9)	79.7
O−Si−Cl1	88.9(1)	104.4	89.5	90.5(1)	95.7
O−Si−Cl2	117.8(1)	115.2	117.0	113.9(1)	114.6
O−Si−Cl3/H1	131.0(1)	113.1	131.4	129.8(9)	126.1
O−Si−N	84.4(1)	68.5	84.4	84.9(1)	80.4
Cl1−Si−Cl2	111.0(1)	105.4	95.2	85.7(1)	99.9
Cl1−Si−Cl3/H1	92.1(1)	107.1	92.0	90.0(9)	97.0
Cl2−Si−Cl3/H1	94.7(1)	110.8	111.2	115.9(9)	114.3
C2−N−Si	100.7(1)	87.3	100.9	102.8(1)	100.5
C3−N−Si	118.5(1)	120.1	118.4	117.6(1)	118.1
C4−N−Si	111.4(2)	115.3	110.8	106.9(1)	105.7

Both molecules adopt five-membered ring structures with intramolecular dative Si−N bonds. The molecules can be considered monomeric, as all intermolecular distances are longer than the sum of the van der Waals radii of the respective atoms. The five-membered rings exhibit "open envelope" conformations with the nitrogen atoms positioned at the tip of the envelope (Figures 1 and 2).

The strong Si−N interactions result in short Si−N distances of 2.060(2) Å in **1** and 2.037(2) Å in **2**. Note that in **1**, with a silicon atom substituted by three chlorine atoms, the Si−N distance is 0.023 Å longer than in **2**, which has a silicon atom substituted by only two chlorine atoms. Because of the larger number of electronegative substituents in **1**, one should expect a higher positive partial charge at this silicon atom, making it more electrophilic and therefore leading to a stronger interaction with the Lewis-basic nitrogen atom.

However, the steric repulsion between the chlorine atoms and the methyl groups of the dimethylamino function does not allow the Si−N distance in **1** to become as short as in **2**, where only one pair of such repulsive interactions is present. This repulsion can be described in terms of intramolecular Cl···H contacts. In **1**, four Cl···H distances below 3 Å (Cl2−H2B, 2.98 Å; Cl2−H4C, 2.69 Å; Cl3−H3C, 2.69; Cl3−H4B, 2.99 Å) are found (Figure 1), whereas in **2**, only two such close Cl···H contacts are observed, and only one of them is below 3 Å (Cl2−H3C, 2.74; Cl2−H2B, 3.03 Å; Figure 2). These values are based on calculated positions of the hydrogen atoms at the carbon atoms.

There are also close distances between non-hydrogen atoms, including Cl2···N (2.980 Å), Cl2···C3 (3.141 Å), Cl3···N (2.897 Å), and Cl3···C4 (3.047 Å) for **1**, which are smaller than the sum of the corresponding van der Waals

radii.[17] Again in **2**, these steric repulsions are less pronounced due to the presence of only one chlorine atom interacting with the dimethylamino function, and the close non-hydrogen atoms distances are consequently larger [Cl2···N (2.993 Å), Cl2···C3 (3.180 Å)].

Anglada et al. have analyzed several silicon compounds with dative Si−N bonds by means of quantumchemical methods and stated that the length of the Si−N bond is shorter as the number of electron-withdrawing groups on silicon increases.[18] They also confirmed earlier experimental findings that the position of the electron-withdrawing group at silicon relative to the donor (apical positions) strongly influences the strength of the Si−N interaction (apicophilicity).[19] The first point concerning a high number of electronegative Si substituents is in contradiction to the results presented here, that a Cl_3Si group is a less effective acceptor than a Cl_2HSi group. The steric effects of three Cl substituents seem to overcompensate the electronic effects. A similar set of results was also found for $Cl_3SiONMe_2$,[20] $Cl_2HSiONMe_2$,[21] and $ClH_2SiONMe_2$[7] (other examples are $Cl_xH_{3-x}GeONMe_2$[22] and $(Me_2NO)_2SiCl_xH_{2-x}$[20,23]), but in an even more pronounced form: the Si−N distance in $ClH_2SiONMe_2$ is 0.41 Å shorter than in $Cl_3SiONMe_2$ in the solid state; the Si−O−N angle, an important feature for the determination of the relative strength of the Si···N interaction in such Si−O−N compounds, is 24° smaller in $ClH_2SiONMe_2$. However, these examples, as well as the structures of **1** and **2**, support the view that the electronic nature of the substituents in an anti position at silicon relative to the dative bond is very important for an enhanced Si−N interaction.[7]

The coordination spheres about the silicon centers in **1** and **2** are close to trigonal bipyramidal. The apical positions are occupied by the nitrogen atom and Cl1. The anti position of the nitrogen atom relative to Cl1 leads to a longer Si−Cl1 bond compared to the bonds Si−Cl2 and Si−Cl3. This effect can also be seen to be the reason for a shorter Si−N distance in **2** (2.037(2) Å and 2.060(2) Å in **1**), leading to a longer Si−Cl1 bond in **2** (2.180(1) Å) than in **1** (2.157(1) Å). The sum of the angles about the silicon atom, involving the atoms Cl2, Cl3, and O, is 359.8° in **1** and 359.6° in **2**, which is close to the 360° expected for ideal trigonal bipyramidal coordination spheres.

NMR Spectroscopy Studies. In addition to standard ^1H, ^{13}C, and ^{29}Si NMR measurements for the characterization of **1**, **2**, and **3**, we also performed variable-temperature $^1H,^{29}Si$-HMBC-NMR (HMBC = heteronuclear multiple bond coherence) experiments. The resulting data are shown in Tables 3−5 (the spectra are provided in the Supporting Information to this manuscript). At ambient temperatures, **1**, **2**, and **3** give ^{29}Si chemical shifts and $^1J_{SiH}$ coupling constants, which indicate the existence of a five-membered ring conformer in solution (Table 3).

Table 3. Selected NMR Chemical Shifts (ppm) and Coupling Constants (Hz) of $Cl_3SiOCH_2CH_2NMe_2$ (**1**), $Cl_2HSiOCH_2CH_2NMe_2$ (**2**), and $ClH_2SiOCH_2CH_2NMe_2$ (**3**) in C_6D_6 at Ambient Temperature[a]

compound	δ^1H (Si*H*)	$^1J_{SiH}$	^1H (NCH_3)	$\delta(^{13}C)$ (NCH_3)	$\delta(^{13}C)$ (NC*H*)	$\delta(^{29}Si)$
1			1.90	45.4	57.2	−72
2	5.64	376	1.66	43.6	55.5	−75
3	5.15	293	1.46	43.0	57.1	−71

[a] For comparison: the solid-state NMR (MAS) value for **1** is −95 ppm.

Scheme 2. Equilibrium between Open Chain and Ring Conformers of **1**, **2**, and **3**

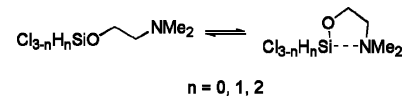

This is very likely to happen, since the molecules are potentially highly flexible and can form five-membered rings by a dative intramolecular Si−N interaction (Scheme 2).

As the change between the two mentioned conformers can be expected to be rapid at ambient temperatures, this leads to an averaging of the NMR chemical shifts of the open-chain and ring conformer on the NMR time scale. These chemical shifts may be compared with those of $Cl_3SiOCH_2CH_3$ (−38.3 ppm) and $Cl_2HSiOCH_2CH_3$ (−48 ppm), which have very similar surroundings about the silicon atoms but, in the absence of donor functions, are clearly tetra-coordinate. Relative to these compounds, **1** and **2** (and also **3**) exhibit strongly upfield-shifted ^{29}Si NMR signals. The NMR data of $Cl_3SiOCH_2CH_3$ were known;[24] $Cl_2HSiOCH_2CH_3$ was synthesized and measured for this purpose in this work (see Experimental Section).

The temperature dependence of the equilibrium as depicted in Scheme 2 becomes evident from the results of NMR experiments at variable temperatures. Expectedly, upon increasing the temperature, the equilibrium between the two conformers of both **1** and **2** shifts to the side of the open-chain conformer and the experimental chemical shift comes closer to the chemical shift of the reference compounds $Cl_3SiOCH_2CH_3$ and $Cl_2HSiOCH_2CH_3$. At lower temperatures, the equilibrium shifts to the side of the ring conformers. For **1**, it finally converges (see Table 4) at a chemical shift obtained by solid-state ^{29}Si MAS NMR (−95 ppm), as the solid solely contains ring conformers (see the crystal structure).

The ^1H NMR spectra also represent the strong temperature dependence of the conformer equilibria. The alkyl functions adjacent to the nitrogen atom experience a strong upfield shift for **1** and **2** upon decreasing the temperature (Tables 4 and 5). In the case of compound **2**, a splitting of the $\delta(^1H,CH_2N)$ and $\delta(^1H,CH_3N)$ signals is observed at temperatures lower than 203 K. This is due to a rapid interconversion between open-chain and ring conformers of **2** at higher

(17) Emsley, J. *The Elements*; Clarendon Press: Oxford, U.K., 1991.
(18) Anglada, J. M.; Bo, C.; Bofill, J. M.; Crehuet, R.; Poblet, J. M. *Organometallics* **1999**, *18*, 5584.
(19) Corriu, R. J. P.; Kpoton, A.; Poirier, M.; Royo, G.; de Saxcé, A.; Young, J. C. *J. Organomet. Chem.* **1990**, *395*, 1.
(20) Losehand, U.; Mitzel, N. W.; Rankin, D. W. H. *J. Chem. Soc., Dalton Trans.* **1999**, 4291.
(21) Vojinović, K.; Mitzel, N. W.; Foerster, T.; Rankin, D. W. H. *Z. Naturforsch.* **2004**, *59b*, 1505.
(22) Mitzel, N. W.; Losehand, U. *Eur. J. Inorg. Chem.* **1998**, 2023, and ref 6.
(23) Mitzel, N. W.; Losehand, U.; Hinchley, S. L.; Rankin, D. W. H. *Inorg. Chem.* **2001**, *40*, 661.
(24) Kintzinger, J.-P.; Marsmann, H.; *Oxygen-17 and Silicon-29 NMR*; Springer: Berlin, 1981.

Table 4. Temperature Dependence of the ^{29}Si and the $^{1}H(NCH_3)$ Chemical Shifts of **1** in D_8-Toluene Solution[a]

T/K	$\delta(^{29}Si)$	$\delta(^{1}H)(NCH_3)$
353	−44.3	1.96
333	−47.5	1.92
323	−49.8	1.92
313	−53.4	1.87
298	−61.3	1.83
283	−72.0	1.82
263	−78.7	1.74
243	−87.8	1.70
223	−93.0	1.70

[a] The value for the reference compound $Cl_3SiOCH_2CH_3$ at RT is −38.3 ppm. The value for **1** in the solid state (MAS-NMR) at ambient temperature is −95 ppm.

Table 5. Temperature Dependence of the ^{29}Si, $^{1}H(SiH)$, $^{1}H(NCH_3)$, and $^{1}H(NCH_2)$ Chemical Shifts and the $^{1}J_{SiH}$ Coupling Constant in D_8-Toluene Solution for Compound **2**[a]

T/K	$\delta(^{29}Si)$	$\delta(^{1}H)$ (SiH)	$^{1}J_{SiH}$/Hz	$\delta(^{1}H)(NCH_2)$	$\delta(^{1}H)(NCH_3)$
368	−58.9	5.57	370	2.04	1.82
353	−62.8	5.56	372	1.98	1.76
333	−67.6	5.57	373	1.93	1.70
313	−71.3	5.57	374	1.89	1.65
298	−73.9	5.58	374	1.86	1.61
283	−76.2	5.56	374	1.86	1.58
263	−78.3	5.59	374	1.83	1.55
243	−78.7	5.61	374	1.80	1.50
223	−80.6	5.68	374	1.79	1.49
203	−81.6	5.74	374	1.48	1.48
193	−81.8	5.76	374	2.15,1.43	1.61,1.33
183	−82.1	5.79	374	2.21,1.42	1.63,1.31
178	−82.2	5.80	374	2.22,1.42	1.63,1.31

[a] The value $\delta(^{29}Si)$ for the reference compound $Cl_2HSiOCH_2CH_3$ at RT is −48 ppm.

temperatures (243−368 K). The ^{29}Si NMR chemical shift tells that at these temperatures the spectra are no longer dominated by the ring conformer. At 298 K, the "normal" splitting of the signals is observed as expected, that is, a singlet for the $N(CH_3)_2$ moiety and triplets for the CH_2 functions.

At temperatures between 223 and 203 K, the ring closure can be considered as almost completed, because the ^{29}Si NMR chemical shift has converged with the temperature. However, at these temperatures, only one ^{1}H NMR signal is observed for the CH_2 and CH_3 groups attached to nitrogen. Consequently, it has to be assumed that a rapid pseudorotation takes place at the silicon atom, which accounts for the nonchirality of **2** on the time scale of the NMR experiment. This pseudorotation takes place while the Si−N bond is intact. However, at temperatures lower than 203 K, separate signals for each proton of the NCH_2 units and the two methyl groups are observed. Therefore, it has to be assumed that, at these temperatures, the conformation at the silicon atom is also frozen, and pseudorotation grinds to a halt. Dynamical behavior like this has been observed before for penta- and tetra-coordinate silicon compounds without rings.[25]

We have performed $^{1}H,^{29}Si$-HMBC-NMR experiments for **1** and **2** at variable temperatures. This two-dimensional NMR method correlates chemical shifts of nuclei, which interact by scalar coupling. Information on atom connectivity through few bonds is therefore accessible, as longer distances correspond to negligible coupling constants.

In the case of **1**, we observed only one cross peak at a high temperature (353 K), which describes the correlation of the chemical shift of the ^{29}Si nuclei with that of the protons of the OCH_2 groups. Further cross-peaks were observed at lower temperatures, corresponding to correlations between the silicon nuclei and the CH_2N and NCH_3 groups. The intensities of these cross-peaks increase with lower temperatures. Since the number of bonds alongside the molecular backbone of an open-chain conformer is too large to allow for such an interaction, the experiment proves the existence of a Si−N bond in **1** and moreover the existence of electron density between Si and N atoms mediating this coupling.

A similar situation is found for compound **2**. In these spectra, we observed cross-peaks between the chemical shifts of the silicon atom and the alkyl groups at nitrogen at even higher temperatures (368 K). Again, and in analogy to **1**, this proves the existence of a Si−N bond also in **2**. At lower temperatures, the integral of these cross-peaks decreases. It is likely that this is an effect of the ring conformation, as torsion angles can be adopted which are responsible for small coupling constants according to the Karplus relation.[26,27] To the best of our knowledge, these VT-HMBC experiments are the first that identify dative bonds in solution.

Thermodynamic Properties of 1 and 2. Because of the temperature dependence of the ^{29}Si chemical shifts of **1** and **2**, it should be possible to draw conclusions about thermodynamic properties. In the preceding section, we have proved that at high temperatures (about 350 K) the open-chain conformers of **1** and **2** have a high abundance in solution, while at low temperatures (<220 K), the ring conformer is dominant. The experimentally observed chemical shift can be expressed as an averaging of the contributions of the individual conformers.

$$\delta_{exp} = X_o \cdot \delta_o + X_r \cdot \delta_r \tag{1}$$

Herein X_o and X_r describe the mole fractions of the open chain and ring conformers, while δ_o and δ_r describe their ^{29}Si NMR chemical shifts. The equilibrium constant K of the interconversion of the open chain into the ring conformer (Scheme 2) is then given by the following equation:

$$K = \frac{C_r}{C_o} = \frac{X_r}{X_o} = \frac{1 - X_o}{X_o} = \frac{1 - \dfrac{\delta_{exp} - \delta_r}{\delta_o - \delta_r}}{\dfrac{\delta_{exp} - \delta_r}{\delta_o - \delta_r}} \tag{2}$$

C_r and C_o are the concentrations of the conformers; δ_{exp} is the experimentally observed chemical shift. This leads to

$$\delta_{exp} = \frac{\delta_o + K \cdot \delta_r}{1 + K} \tag{3}$$

The equilibrium constant K is expressed as a function of the

(25) Corriu, R. J. P.; Kpoton, A.; Poirier, M.; Royo, G. *J. Organomet. Chem.* **1984**, *277*, C25.

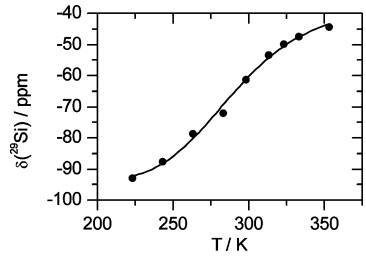

Figure 3. Fitting of the derived function for δ_{exp} to the experimental ^{29}Si NMR chemical shifts of **1**.

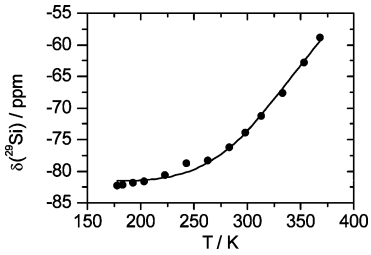

Figure 4. Fitting of the derived function for δ_{exp} to the experimental ^{29}Si NMR chemical shifts of **2**.

different partition functions of the sum of various open-chain conformers (q_o) and the ring conformer (q_r).

$$K = \frac{q_o}{q_r} e^{\frac{-\Delta G}{RT}} \quad (4)$$

As neither q_o nor q_r are known, an established approximation is applied, as is used for the description of a reaction A $\rightleftarrows$ B, where many states equally spaced in energy (ε) for B are considered with $m = \varepsilon/k$ (k = Boltzmann constant).[28] Here, the assumption is (a) that only one energy level for the sole ring conformer is relevant, and thus q_r equals unity, and (b) that q_o is a product $m \cdot T$, with T being the temperature and m a factor accounting for the existence of a variety of open-chain conformers, which are close in energy. Factor m is introduced to account for the above-mentioned approximations of the thermodynamic model. Models neglecting this temperature dependence in the term $m \cdot T$ cannot be fitted to the experimental data.

The resulting function for fitting is

$$\delta_{exp} = \frac{\delta_o + m \cdot T \cdot e^{\frac{-\Delta G}{RT}} \cdot \delta_r}{1 + m \cdot T \cdot e^{\frac{-\Delta G}{RT}}} \quad (5)$$

This function contains four parameters (δ_o, δ_r, m, and ΔG) and one variable (T). It can be fitted to the experimental chemical shifts (Figures 5 and 6).

The fitting generates parameter values that are very well in the range of expected values. The quality of the fits can be judged from Figures 3 and 4. For **1**, ΔG is calculated to be -28.8 ± 3.9 kJ·mol^{-1}, $\delta_r = -94 \pm 2$ ppm, and $\delta_o = -36 \pm 5$ ppm. From the MAS NMR experiment and by comparison to the reference compound, we had expected the values $\delta_r = -95$ ppm and $\delta_o = -38$ ppm, so that the formula for δ_{exp} (eq 5) seems to describe the experimental data very well. For compound **2**, we expected values of $\delta_r = -84$ ppm and $\delta_o = -48$ ppm. The fitting of δ_{exp} to the experimental values resulted in $\Delta G = -22.3 \pm 0.4$ kJ·mol^{-1}, $\delta_r = -82 \pm 1$ ppm, and $\delta_o = -33 \pm 4$ ppm, so only the latter deviates from the reference value but is very close to the value of **1** (−38 ppm).

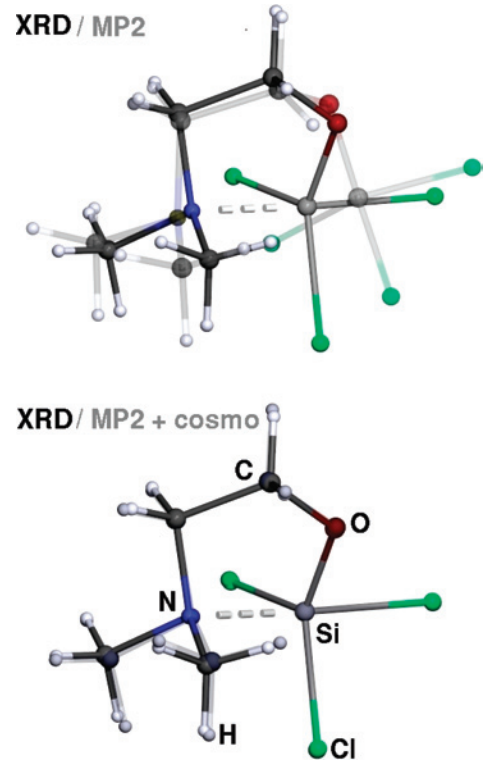

Figure 5. Superposition of the molecular structure of **1** in the solid state (normal print) with the results of MP2/TZVPP calculations (faint print). The upper part represents the results without application of a dielectric continuum model (XRD/MP2); the lower part shows the excellent fit resulting from the application of a dielectric continuum model using conductor-like screening model (COSMO; XRD/MP2+cosmo). The main deviations that can be seen are due to the inappropriate description of hydrogen atom positions by X-ray diffraction.

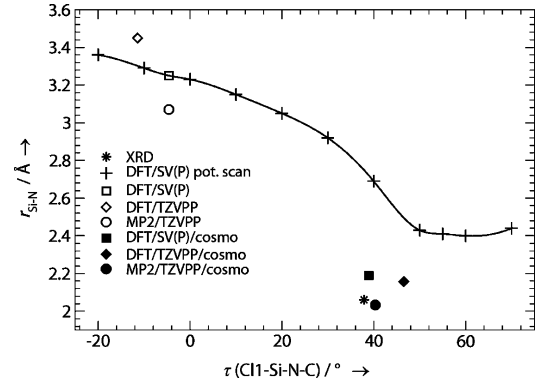

Figure 6. Dependence of the Si−N distance on the torsional angle Cl(1)−Si−N−C(2) in **1**. The plot shows the results of relaxing geometries at the DFT/SV(P) level of theory with a fixed torsional angle. In addition, the results of other calculations are shown with these parameters obtained at the optimized global energy minima.

(26) Karplus, M. *J. Chem. Phys.* **1959**, *30*, 11–15.
(27) Karplus, M. *J. Chem. Phys.* **1963**, *85*, 2870.
(28) Atkins, P. W.; *Physical Chemistry*, 4th ed.; Oxford University Press: Oxford, 1981.

During the conversion of the open-chain into the ring conformer, some ring strain is built up, but the attractive interaction of the silicon and nitrogen atom overcompensates this energy. The ΔG values describe the sum of these processes, but they are dominated by the strength of the dative Si−N interactions and therefore are good first approximations for them.

The parameter m, which was introduced to account for the mixture of open-chain conformers, was fitted to values of $m = 2.3 \times 10^{-8} \pm 3.9 \times 10^{-8}$ K^{-1} for **1** and $m = 2.2 \times 10^{-6} \pm 9.0 \times 10^{-7}$ K^{-1} for **2**; that is, in terms of standard deviation, this parameter is meaningless.

A direct comparison to literature data is to the best of our knowledge not possible, since no such examinations have been performed yet. However, Corriu and co-workers have derived activation enthalpies (ΔG^*) of chiral δ-donor substituted silanes by examining the coalescence of the ^{1}H NMR signals corresponding to cleavage of silicon−nitrogen bonds. Values from about 40 kJ·mol^{-1} to about 90 kJ·mol^{-1} were derived by this method.[19,29] In these works, rather rigid molecules incorporating phenyl or naphtyl backbones were analyzed.

In the near future, we want to demonstrate the broader applicability of this procedure, in which experiments (VT-NMR), which are fairly easy to carry out, can be used to deduce thermodynamic data such as reaction enthalpies and individual chemical shifts of components in chemical equilibria.

Quantum Chemical Calculations. In order to get a more detailed description of bonding in **1** and **2**, we have calculated the structures of these molecules at the MP2/TZVPP level of theory. Surprisingly, these calculations lead to two very different results. For **2**, the calculated structure of the free molecule is already very close to the one adopted in the solid state, described above. The values for the Si···N length are expectedly predicted somewhat larger for the free molecule (2.235 Å) than for the solid state [2.037(2) Å], as these effects are established and due to the interaction of the molecules' dipole moment with the polar surroundings.[30] The molecular dipole moment itself is dependent on the strength of the Si···N interaction. The partial dative bonds are said to be "driven towards completion" by inclusion of the molecule in solid-state surroundings.[28] The remaining geometry parameters are well predicted from theory, as can be seen from Table 2.

In contrast to the situation in **2**, there is a large discrepancy between the calculated geometry of the free molecule and the solid-state structure of **1** (see Figure 5). The Si···N distance is more than 1 Å longer in the calculations for the free molecule than in the crystal structure. This is an unusually large difference for such systems. The geometry of this free molecule is such that it adopts a conformation which brings the chlorine substituents at silicon and the methyl groups at nitrogen together in an almost eclipsed conformation when viewed along the Si−N vector. It may be concluded that this conformation does not allow the silicon and nitrogen atoms to approach each other close enough to form a reasonably strong dative bond.

In order to account for the polarity of the surrounding in the solid state, we performed dielectric continuum model calculations with the conductor-like screening model (COSMO)[31] routine implemented in the ORCA program at the MP2/ZVPP level of theory.[32] The solid-state effects were modeled by choosing an infinite dielectricity constant ε. In fact, the geometry for **1** obtained in this way comes very close to that found experimentally in the solid state. The quality of these calculations can be assessed graphically from Figure 5, showing a superposition of the crystal structure molecular geometry with the calculations of the free molecule without and with application of this dielectric continuum model. In this latter geometry, the whole backbone Si−O−C−C−N adopts a conformation, which arranges the chlorine substituents at silicon and the methyl groups at nitrogen in an almost staggered conformation, so that repulsions are minimized and the Si and N atoms can come close enough to form a dative Si···N interaction. The deformation of the molecular backbone can be described by a torsion about the Si−N axis, and the torsional angle Cl(2)−Si−N−C(2) is a good measure for this. Figure 6 shows the Si−N distance as a function of this torsional angle, as obtained by running several DFT calculations with a fixed torsion angle. In fact, it shows how the molecule has to be deformed until the formation of the Si−N bond can release energy.

Although the behavior of **1** and **2** in solution and the solid state is quite comparable, the substantial differences in bonding between these two compounds as free molecules raise the question of their origin, and thus we have undertaken analyses of the electron density topologies of **1** and **2**.

Topology of the Electron Density. The quantum theory of atoms in molecules (QTAIM)[33] is often used to characterize weak molecular interactions in terms of atomic interaction lines (also called bond paths) and bond critical points (BCPs), but also by a series of other descriptors.[34] We have recently shown that dative bonds between silicon and nitrogen atoms are not always described by QTAIM with the appearance of atomic interaction lines or bond critical points. In fact, the systems $(F_3C)F_2SiONMe_2$[5] and $F_3SiONMe_2$[8] are represented by QTAIM as nonring systems despite the presence of relatively short Si···N distances (less than 2 Å) and acute angles at the oxygen atoms (less than 80°) in the three-membered SiON rings. It was thus of interest to see the electron density topology in **1** and **2**, which also have X_3SiO units interacting with NMe_2 groups, but in a larger ring

(29) Carré, F.; Corriu, R. J. P.; Kpoton, A.; Poirier, M.; Royo, G.; Young, J. C. *J. Organomet. Chem.* **1994**, *470*, 43.
(30) Leopold, K. R.; Canagaratna, M.; Phillips, J. A. *Acc. Chem. Res.* **1997**, *30*, 57. (b) Jiao, H.; Schleyer, P. v. R. *J. Am. Chem. Soc.* **1994**, *116*, 7429.
(31) Schäfer, A.; Horn, H.; Ahlrichs, R. *J. Chem. Phys.* **1992**, *97*, 2571.
(32) Sinnecker, S.; Rajendran, S.; Klamt, A.; Diedenhofen, M.; Neese, F. *J. Phys. Chem. A* **2006**, *110*, 2235.
(33) Bader, R. F. W. *Atoms in Molecules - A Quantum Theory*; Oxford University Press: Oxford, U.K., 1990.
(34) Matta, C. M.; Boyd, R. J. *The Quantum Theory of Atoms in Molecules: From Solid State to DNA and Drug Design*; Wiley-VCH: New York, 2007.

Table 6. Electron Density Topology Parameters for Selected Bonds in **1** in the Calculated Ground State As Obtained at the MP2/TZVPP Level of Theory[a]

A···B	d(A−BCP)	d(B−BCP)	$\rho(r_{BCP})$	$\nabla^2\rho(r_{BCP})$	ε
Cl(2)···H	1.768	1.500	0.05	−0.17	4.45
Cl(3)···C(4)	1.777	2.008	0.05	−0.17	2.41
Si−Cl(1)	0.731	1.311	0.69	−1.56	0.04
Si−Cl(2)	0.728	1.311	0.70	−1.70	0.04
Si−Cl(3)	0.731	1.310	0.69	−1.59	0.01
Si−O	0.664	0.963	0.96	−5.97	0.10
O−C(1)	0.915	0.509	1.58	2.59	0.05
C(1)−C(2)	0.766	0.746	1.72	3.92	0.02
N−C(3)	0.870	0.584	1.83	4.47	0.02
N−C(4)	0.867	0.588	1.83	4.37	0.05
N−C(2)	0.858	0.595	1.85	4.22	0.15

[a] The values given are the distances of the bond critical points (BCP) to the nuclear positions along the bond paths (in Å), the electron densities $\rho(r_{BCP})$ (in ε Å^{-3}), and the values of the Laplacians $\nabla^2\rho(r_{BCP})$ (in e Å^{-5}) and the ellipticities of the interaction at the BCPs.

Table 7. Electron density topology parameters for selected bonds in **2** in the calculated ground state as obtained at the MP2/TZVPP level of theory[a]

A···B	d(A−BCP)	d(B−BCP)	$\rho(r_{BCP})$	$\nabla^2\rho(r_{BCP})$	ε
Si···N	0.868	1.376	0.35	−0.36	1.34
Cl(2)···H	1.648	1.213	0.09	−0.28	0.81
Si−Cl(1)	0.747	1.355	0.61	−1.25	0.04
Si−Cl(2)	0.743	1.338	0.63	−1.36	0.08
Si−H	0.708	0.754	0.85	−1.54	0.05
Si−O	0.677	0.989	0.88	−4.90	0.10
O−C(1)	0.913	0.501	1.72	3.43	0.07
C(1)−C(2)	0.756	0.767	1.73	4.09	0.07
N−C(3)	0.887	0.577	1.78	4.21	0.02
N−C(4)	0.882	0.587	1.78	4.14	0.04
N−C(2)	0.882	0.582	1.797	4.22	0.04

[a] The values given are the distances of the bond critical points (BCP) to the nuclear positions along the bond paths (in Å), the electron densities $\rho(r_{BCP})$ (in e Å^{-3}), and the values of the Laplacians $\nabla^2\rho(r_{BCP})$ (in e Å^{-5}) and the ellipticities of the interaction at the BCPs.

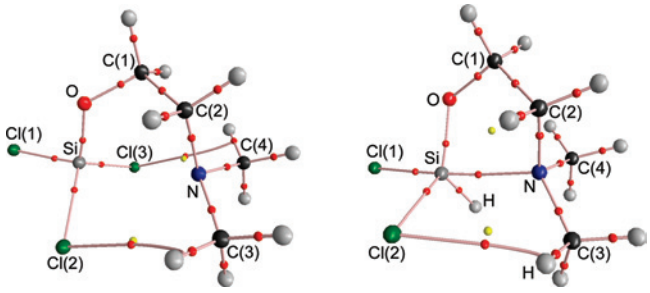

Figure 7. Molecular graphs as obtained by analysis of the electron densities of **1** (left) and **2** (right) obtained at the MP2/TZVPP level of theory. The graphs show atom positions, atomic interaction lines, bond-critical points (in red), and ring-critical points (in yellow).

system. The analyses are also interesting from the point that **1** and **2** are similar in their constitution, but theory predicts very different structures for the free molecules. According to QTAIM, a topology analysis is only valid for equilibrium structures, and thus only the electron densities of the free molecules of **1** and **2** calculated from the wave functions obtained at the MP2/TZVPP level of theory were analyzed, and not so the COSMO-corrected structures. Selected results are listed in Tables 6 and 7; the molecular graphs resulting from the localization of atomic interaction lines are shown in Figure 7, and the electron density and Laplacian maps in the SiON planes are displayed in Figure 8.

Except the Si···N interactions, the atomic interaction lines derived from the charge densities of **1** and **2** recover the molecular graphs drawn from classical chemical considerations. For **2**, the bonding interaction between the Si and N atoms corresponding to a dative bond is found, but not so for **1**. Most of the bonds in **1** and **2** show the typical values of the descriptors used to characterize their nature in bonding (Tables 6 and 7). The C−C and N−C bonds have all high electron densities and negative Laplacian values at their BCPs, indicating their covalent nature. In contrast, the Si−H, Si−O, and Si−Cl bonds have values of less than half the density of the former at their BCPs and positive Laplacians. This is indicative for bonds with a high degree of ionic bonding (closed-shell interactions). The Si···N interaction in **2** is characterized by a BCP with an electron density of 0.35 e Å^{-3}, which is about half that of the Si−H and Si−Cl bonds, and a positive Laplacian value, showing the closed-shell nature of this interaction. Of note is the high ellipticity at the BCP of the Si···N interaction, a fact that was already noted for the Si···N interaction of the cyclic conformer of $H_3SiCH_2CH_2CH_2NMe_2$.[13] It is also interesting to compare this density value to that of the midpoint of the Si···N vector in **1**, which is very low at 0.013 e Å^{-3}.

In this respect, the electron density topology is similar to that of other hypervalent silicon compounds such as the hexacoordinate silicon compound difluorobis[*N*-(dimethylamino)phenylacetimidato-*N*,*O*]silicon with a SiO_2F_2 core plus two nitrogen donor substituents recently investigated by Stalke et al.[35] As in the solid state of **1** and **2**, and in the calculations of free **2**, this compound also has strong Si···N interactions, and consequently we find electron density values at the BCP of the Si···N bonding interaction for **2** at 0.35 e Å^{-3} {compare difluorobis[*N*-(dimethylamino)phenylacetimidato-*N*,*O*]silicon with 0.50 e Å^{-3} and the very weak interaction in $H_3Si(CH_2)NMe_2$ at 0.15 e Å^{-3}}.[13]

Both Laplacian plots of **1** and **2** show the local charge concentrations at the nitrogen atom, which correspond to their lone pair of electrons. In **2**, this is pointing almost straight to the silicon center, which is charge-depleted, whereas in **1**, there is some deviation of this orientation from the Si−N vector.

In both compounds, there are additional atomic interaction lines according to QTAIM. Namely, this is an interaction line between the gauche-positioned chlorine atom in **2** and a hydrogen atom of the methyl group, while for **1** there is also such an interaction line and one, on the other side of the molecule, between a chlorine atom and a carbon atom. All three interaction paths of this type are relatively straight between the BCP and the chlorine atom but show extreme curvatures close to the C−H bonds. They all have very low electron densities at their BCPs (0.09 e Å^{-3} in **2** and 0.05 e Å^{-3} in **1**). Note that both the Cl···H and Cl···C interactions are characterized by unusually high ellipticities at their BCPs.

At present, there is an intense debate about such interactions in the literature, whether they are of an attractive

(35) Kocher, N.; Henn, J.; Gostevskii, B.; Kost, D.; Kalikhman, I.; Engels, B.; Stalke, D. *J. Am. Chem. Soc.* **2004**, *126*, 5563.

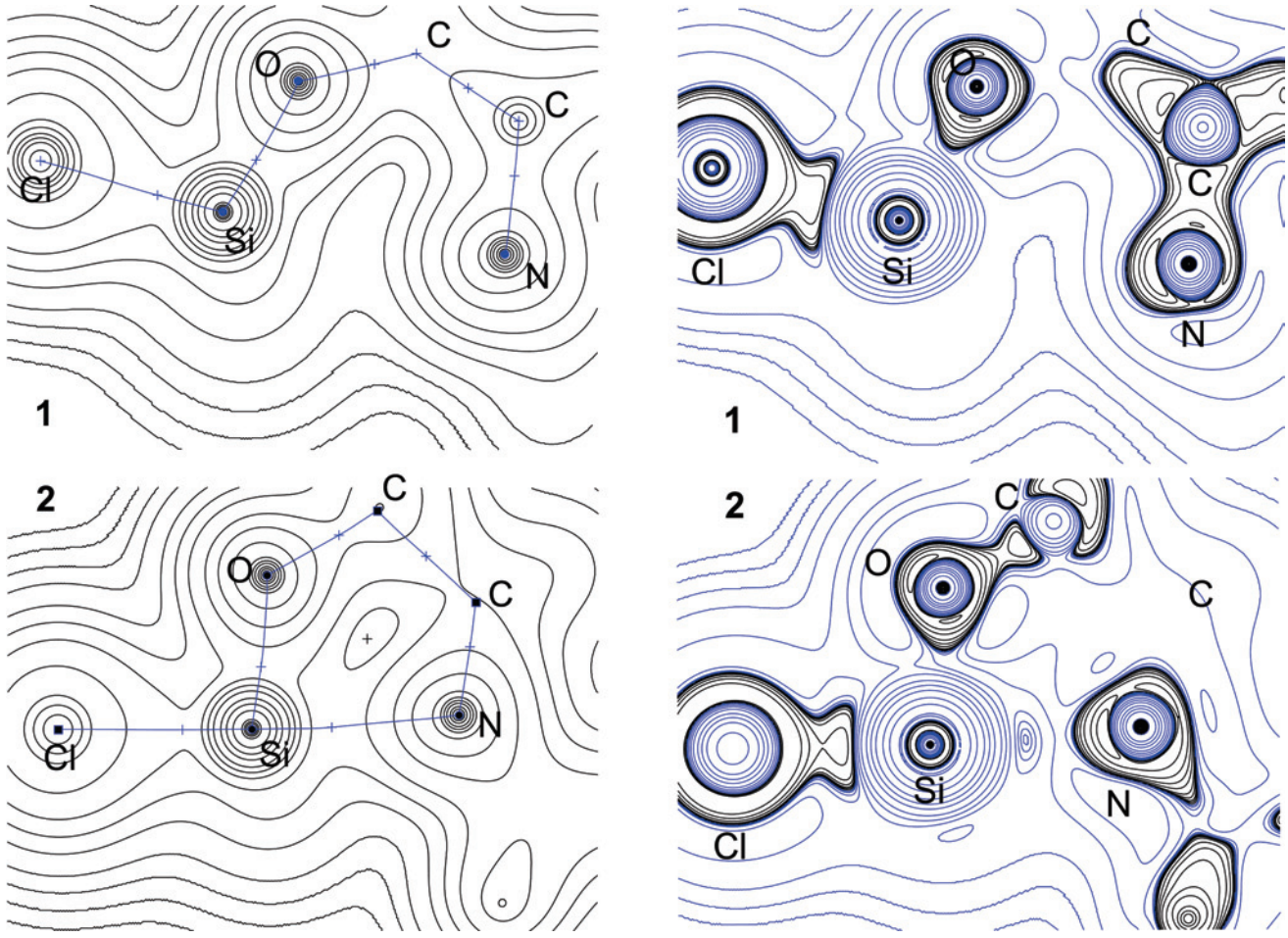

Figure 8. Calculated electron density maps (left) and Laplacians of electron density (right) in the SiON planes for **1** (above) and **2** (below) as obtained at the MP2/TZVPP level of theory. The density maps show atomic interaction lines and bond-critical points; lines are printed at values of 0.002×10^n, 0.004×10^n and 0.008×10^n *e* Å^{-1}, $n = 0, 1, 2, 3,...$). The Laplacian lines are printed at values of $\pm 0.002 \times 10^n$, $\pm 0.004 \times 10^n$, and $\pm 0.008 \times 10^n$ *e* Å^{-1}, $n = 0, 1, 2, 3,...$), whereby blue lines represent positive values and black lines represent negative values.

(bonding) or a repulsive nature.[36] In particular, the H···H interactions in the biphenyl system are under controversial discussion.[37]

In our cases of **1**, we could conclude that the Cl···H and Cl···C interactions in the free molecule serve as forces preorganizing the structure, so that these position the Si and N atoms in a way that, upon the action of external fields, the Si···N interaction can be strengthened. However, as was demonstrated with the interplay between torsion and Si···N interaction displayed in Figure 6, it is then necessary to deform the molecular backbone in order to allow for the formation of a Si···N bond, as observed in solid **1**. This can thus not be explained by the Cl···H and Cl···C interactions in terms of attractive forces but rather by their repulsive nature.

In **2**, where only one such Cl···H interaction is found in the charge density topology, the Si−N bond is a fully operative dative bond, also recognized by the charge density topology analysis. In contrast, compound **1** has two such interactions, the Cl···H and Cl···C interactions, and despite a more electronegatively substituted silicon atom, no marked contribution of a Si···N dative bond. The interaction between Si and N atoms in the free molecule is so long and weak that no atomic interaction line is found in the charge density map. This is a strong indication that the Cl···H and Cl···C interactions are of repulsive nature, preventing the Si···N interaction of being formed in the free molecule. However, these repulsive interactions are overridden by external fields, which drive the Si···N interaction to become almost as short as in **2** by mutual dipole stabilization in the solid state. This was modeled by the COSMO calculations and is experimentally verified in the crystal structure but, as said above, requires substantial deformation of the molecular backbone.

Conlusions

In this contribution, we have described the structures of $Cl_3SiOCH_2CH_2NMe_2$ (**1**) and $Cl_2HSiOCH_2CH_2NMe_2$ (**3**), as determined by X-ray diffraction. Compounds **1** and **2** show five-membered ring-shaped molecules in the solid state, exhibiting strong intramolecular dative Si−N bonds with short Si−N distances of 2.060(2) Å (**1**) and 2.037(2) Å (**2**)

(36) Poater, J.; Visser, R.; Solá, M.; Bickelhaupt, F. M. *J. Org. Chem.* **2007**, *72*, 1134.

(37) (a) Matta, C. F.; Hernandez-Trujillo, J.; Tang, T.; Bader, R. F. W. *Chem.—Eur. J.* **2003**, *9*, 1940. (b) Cioslowski, J.; Mixon, S. T. *J. Am. Chem. Soc.* **1992**, *114*, 4382. (c) Cioslowski, J.; Mixon, S. T. *Can. J. Chem.* **1992**, *70*, 443. (d) Haaland, A.; Shorokhov, D. J.; Tverdova, N. V. *Chem.—Eur. J.* **2004**, *10*, 4416. (e) Poater, J.; Solá, M.; Bickelhaupt, F. M. *Chem.—Eur. J.* **2006**, *12*, 2889. (f) Poater, J.; Solá, M.; Bickelhaupt, F. M. *Chem.—Eur. J.* **2006**, *12*, 2902.

in the solid state. By $^{1}H,^{29}Si$-HMBC-NMR experiments, we were able to show that the Si−N bonds also exist in solution, depending on the temperature. So, in solution, an equilibrium between open-chain conformers, without Si−N contacts, and ring conformers was found. At high temperatures, the equilibrium shifts toward the side of the open-chain conformer, while at low temperatures, the equilibrium shifts to the side of the ring conformer. Additionally, we were able to examine dynamic properties of **2** in solution. At high temperatures, this molecule is totally flexible, but at low temperatures, it can be shown that the Si−N bond is fully established, while a pseudorotation on the pentacoordinate silicon center takes place. Upon further cooling, even this pseudorotation is frozen out, so that the conformation of the five-membered ring is fully persistent. We have derived the free enthalpy of conversion of the open-chain conformers of **1** and **2** into the ring conformers from the temperature dependence of the ^{29}Si chemical shift to be $\Delta G = -28.8 \pm 3.9$ kJ·mol^{-1} (**1**) and $\Delta G = -22.3 \pm 0.4$ kJ·mol^{-1} (**2**). Quantum-chemical calculations show the structure of **2** as a free molecule to be similar to that in the crystal with a somewhat shorter Si−N bond in the solid. In contrast, **1** has a very different structure as a free molecule, with the Si−N distance being more than 1 Å longer than in the crystal and with a substantially deviated conformation. The repulsions between Cl and the methyl groups' H and C atoms in **1** are responsible for this. Calculations including corrections according to a dielectric continuum model (COSMO) for mimicking the polar surrounding in the solid state impressively reproduce the geometry found in the crystal structure. Analysis of the bonding situations of the free molecules of **1** and **2** by means of QTAIM reproduces the molecular graphs and shows the presence of a Si−N bond in **2**, but the absence of such in **1**. Atomic interaction lines are found between Cl and the methyl groups' H and C atoms in both compounds. In view of the whole situation described in this paper, these interactions have to be described as repulsive, despite the contrasting interpretation by some authors in related cases.

Acknowledgment. The authors are grateful to the Graduate School of Chemistry at the Westfälische Wilhelms−Universität in Münster (stipend to M.H.) and to Deutsche Forschungsgemeinschaft (SPP 1178 "Experimental Electron Density") for financial support. We thank Dr. A. Hepp for NMR measurements and T. Pape (both Inorganic Chemistry, University of Münster) for data collection for the structure of **1** and Dr. M. Patzschke (Helsinki) for help with ORCA ab-initio calculations.

Note Added after ASAP Publication. There was an error in Figures 4 and 6 published ASAP October 11, 2008; the corrected version published ASAP October 22, 2008.

Supporting Information Available: Additional tables and figures are provided. This material is available free of charge via the Internet at http://pubs.acs.org.

IC801205Q